Velocity-Space Structures of Distribution Function in Toroidal Ion Temperature Gradient Turbulence

T.-H.Watanabe and H.Sugama

National Institute for Fusion Science / The Graduate University for Advanced Studies,
Toki, Gifu, 509-5292, Japan

e-mail contact of main author: watanabe.tomohiko@nifs.ac.jp

Abstract. Velocity-space structures of ion distribution function associated with the ion temperature gradient (ITG) turbulence and the collisionless damping of the zonal flow are investigated by means of a newly developed toroidal gyrokinetic-Vlasov simulation code with high velocity-space resolution. The present simulation on the zonal flow and the geodesic acoustic mode (GAM) successfully reproduces the neoclassical polarization of trapped ions as well as the parallel phase mixing due to passing particles. During the collisionless damping of GAM, finer-scale structures of the ion distribution function in the velocity space continue to develop due to the phase mixing while preserving an invariant defined by a sum of an entropy variable and the potential energy. Simulation results of the the toroidal ITG turbulent transport clearly show generation of the fine velocity-space structures of the distribution function and their collisional dissipation. Detailed calculation of the entropy balance confirms the statistically steady state of turbulence, where the anomalous transport balances with the dissipation given by the weak collisionality. The above results obtained by simulations with high velocity-space resolution are understood in terms of generation, transfer, and dissipation processes of the entropy variable in the phase space.

1. Introduction

Numerical simulations based on the gyrokinetic formalism for drift wave turbulence, such as the ion temperature gradient (ITG) mode [1], have been extensively performed with the aim of understating anomalous transport mechanism in a core region of magnetically confined plasmas. Transport suppression by self-generated zonal flows [2, 3] is one of the important results confirmed by the numerous simulations as well as theoretical investigations. In a high-temperature plasma, where mean-free-paths of ions and electrons are much longer than device sizes, the one-body velocity distribution function, f, is far from the thermal equilibrium with the Maxwellian, F_M. This is why kinetic approaches are indispensable for studying the core turbulent transport. Velocity-space structures of the distribution function and their relation to the turbulent transport, however, have rarely been discussed in the conventional kinetic simulations.

Regarding the velocity-space structures of f in plasma turbulence, it has been theoretically pointed out that, if a steady transport flux is observed in collisionless turbulence driven by constant density or temperature gradients, a quasisteady state should be realized [4–6], where high-order velocity-space moments of the perturbed distribution function δf continue to grow but the low-order ones are constant in average. Here, the deviation of f from the equilibrium is defined by $\delta f \equiv f - F_M$. Our gyrokinetic-Vlasov (Eulerian) simulation manifested existence of the quasisteady state of the collisionless slab ITG turbulence [7], where continuous generation of micro velocity-scale structures of δf through the phase mixing is responsible for the growth of the high-order moments. The quasisteady state is also characterized by a balance between monotonic increase of an entropy variable defined by a square-integral of δf and the turbulent transport. Recently, it has also been shown numerically and analytically how the whole velocity-space spectrum of f from macro to micro scales is determined by processes of the anomalous heat transport, the phase mixing, and the dissipation in the steady state of the weakly collisional slab ITG turbulence [8]. As the macro velocity-space structures of f directly related to the transport flux are hardly influenced in the weak collisionality limit, the transport coefficient asymptotically approaches the value of the collisionless case [8]. It is emphasized

that only a kinetic simulation with high velocity-space resolution and negligible numerical dissipation enables one to quantitatively investigate how the turbulent transport depends on the weak collisionality.

We have now developed a new toroidal gyrokinetic-Vlasov simulation code with high velocity-space resolution [9], which can precisely deal with the phase-mixing processes of f in toroidal configurations. With this code, detailed velocity-space structures produced by collisionless dynamics of the zonal flow [10] and the geodesic acoustic mode (GAM) [11] are successfully simulated and the transport flux in the toroidal ITG turbulence consistent with the entropy balance can be obtained. In this paper, we present the numerical simulation results of the zonal flow dynamics and the ITG turbulent transport in a tokamak configuration, focusing on the velocity-space structures of the ion distribution function.

This paper is organized as follows. After introduction of the physical model in Section 2, the balance equation for the entropy variable in a toroidal flux tube configuration is described in Section 3. In Section 4, we report velocity-space structures of δf during the collisionless damping of GAM associated with the zonal flow, of which the level is considered to be critical to determination of the transport flux in the toroidal ITG turbulence. Nonlinear simulations of the toroidal ITG turbulent transport are shown in Section 5, where the entropy balance and the velocity-space structures of the distribution function are discussed. The results are summarized in Section 6.

2. Model

We consider the gyrokinetic equation [12] for the ion distribution function in the low-β (electrostatic) limit. By applying the flute reduction for a large-aspect-ratio tokamak with concentric circular magnetic surfaces and the major radius R_0, the governing equations are written as

$$\frac{\partial \delta f}{\partial t} + v_\parallel \boldsymbol{b} \cdot \nabla \delta f + \frac{c}{B_0} \{\Phi, \delta f\} + \boldsymbol{v}_d \cdot \nabla \delta f - \mu \boldsymbol{b} \cdot \nabla \Omega_i \frac{\partial \delta f}{\partial v_\parallel} = \left(\boldsymbol{v}_* - \boldsymbol{v}_d - v_\parallel \boldsymbol{b}\right) \cdot \frac{e \nabla \Phi}{T_i} F_M + C\left(\delta f\right) \tag{1}$$

where $\boldsymbol{b}$, B_0, c, Φ, e, and T_i are the unit vector parallel to the magnetic field, magnetic field strength on the magnetic axis, the speed of light, the electrostatic potential evaluated at the guiding center, the elementary charge, and the ion temperature, respectively. The magnetic moment is defined by $\mu \equiv v_\perp^2/2\Omega_i$ with the ion cyclotron frequency $\Omega_i = eB/m_ic$ (m_i is the ion mass). The collision term is shown by $C\left(\delta f\right)$.

In the toroidal flux tube coordinates [13], $x = r - r_0$, $y = \frac{r_0}{q_0}\left[q(r)\theta - \zeta\right]$, and $z = \theta$, [where the safety factor $q(r = r_0) = q_0$ at the minor radius $r = r_0$], background gradients and magnetic shear parameters are assumed to be constant, such that $L_n = -(d\ln n/dr)^{-1}$, $L_T = -(d\ln T_i/dr)^{-1}$, and $q(r) = q_0[1 + \hat{s}(r - r_0)/r_0]$. The poloidal and toroidal angles are denoted by θ and ζ, respectively. The abbreviations are defined by

$$\boldsymbol{b} \cdot \nabla = \frac{1}{q_0 R_0} \frac{\partial}{\partial z} , \quad \{\Phi, \delta f\} = \frac{\partial \Phi}{\partial x}\frac{\partial \delta f}{\partial y} - \frac{\partial \Phi}{\partial y}\frac{\partial \delta f}{\partial x} , \quad B = B_0\left(1 - \frac{r_0}{R_0}\cos z\right) ,$$

$$\boldsymbol{v}_d = -\frac{v_\parallel^2 + \Omega_i\mu}{\Omega_i R_0}\left[\hat{x}\sin z + \hat{y}(\cos z + \hat{s}z\sin z)\right] , \quad \boldsymbol{v}_* = -\hat{y}\frac{cT_i}{eL_nB_0}\left[1 + \eta_i\left(\frac{m_iv^2}{2T_i} - \frac{3}{2}\right)\right] ,$$

where $\eta_i = L_n/L_T$. Unit vectors in the x and y directions are denoted by $\hat{x}$ and $\hat{y}$, respectively. The radially-localized flux tube model enables us to impose the periodic boundary condition

both in the x and y directions so that the spectral method can be applied to calculation of the convection (the Poisson brackets) term in Eq.(1). In the perpendicular wave number space (k_x, k_y), Φ is related to the electrostatic potential, such that

$$\Phi_{k_x,k_y} = J_0(k_\perp v_\perp/\Omega_i)\phi_{k_x,k_y} . \tag{2}$$

Here, J_0 is the zero-th order Bessel function and $k_\perp^2 = (k_x + \hat{s}zk_y)^2 + k_y^2$. The potential acting on particle positions, ϕ_{k_x,k_y}, is determined by the quasi-neutrality condition,

$$\int J_0 f_{k_x,k_y} d^3v - \frac{e\phi_{k_x,k_y}}{T_i} n_0 (1 - \Gamma_0) = n_{e,k_x,k_y} , \tag{3}$$

where the Fourier component of δf is denoted by f_{k_x,k_y}. Also, $\Gamma_0 = e^{-b}I_0(b)$ with $b = (k_\perp v_{ti}/\Omega_i)^2$. The zero-th order modified Bessel function and the ion thermal speed are represented by I_0 and $v_{ti} = \sqrt{T_i/m_i}$, respectively. The electron density perturbation, n_{e,k_x,k_y}, from the total one, n_0, with temperature T_e is assumed to be adiabatic,

$$\frac{n_{e,k_x,k_y}}{n_0} = \begin{cases} \tau\dfrac{e\left(\phi_{k_x,k_y} - \left\langle \phi_{k_x,k_y}\right\rangle\right)}{T_i} & \text{for } k_y = 0 \\[3mm] \tau\dfrac{e\phi_{k_x,k_y}}{T_i} & \text{for } k_y \neq 0 \end{cases}, \tag{4}$$

where $\tau = T_i/T_e$ and $\langle \cdots \rangle$ means the flux surface average defined by

$$\langle A \rangle = \int_{-N_\theta\pi}^{+N_\theta\pi} \frac{A}{B}dz \bigg/ \int_{-N_\theta\pi}^{+N_\theta\pi} \frac{1}{B}dz . \tag{5}$$

The parallel length of the flux tube is set to $2N_\theta\pi$ where the modified periodic boundary condition is used in the z direction [13]. Hereafter, physical quantities are normalized as follows; $x = x'/\rho_i$, $t = t'v_{ti}/L_n$, $v = v'/v_{ti}$, $B = B'/B_0$, $\phi = e\phi'L_n/T_i\rho_i$, and $f = f'L_n v_{ti}^3/\rho_i n_0$, where prime means dimensional quantities and $\rho_i = v_{ti}/\Omega_i$.

3. Entropy Balance

The entropy balance equation (normalized) is derived from Eqs.(1), (3), and (4), such that

$$\frac{d}{dt}(\delta S + W) = \eta_i Q_i + D_i . \tag{6}$$

In the flux tube coordinates, the entropy variable, δS, the potential energy, W, the ion heat transport flux, Q_i, and the collisional dissipation, D_i, are, respectively, defined as

$$\delta S = \sum_{k_x,k_y} \delta S_{k_x,k_y} = \frac{1}{2}\sum_{k_x,k_y}\left\langle \int \frac{|f_{k_x,k_y}|^2}{F_M}d^3v \right\rangle ,$$

$$W = \sum_{k_x,k_y} W_{k_x,k_y} = \frac{1}{2}\sum_{k_x,k_y}\left[\left\langle (1 - \Gamma_0 + \tau)|\phi_{k_x,k_y}|^2 \right\rangle - \tau|\left\langle \phi_{k_x,k_y}\right\rangle|^2\delta_{k_y,0}\right] ,$$

$$Q_i = \sum_{k_x,k_y} Q_{i,k_x,k_y} = \frac{1}{2}\sum_{k_x,k_y}\left\langle ik_y\phi_{-k_x,-k_y}\int v^2 J_0 f_{k_x,k_y}d^3v\right\rangle ,$$

$$D_i = \sum_{k_x,k_y} D_{i,k_x,k_y} = \sum_{k_x,k_y}\left\langle \int\left[\left(J_0\phi_{-k_x,-k_y} + \frac{f_{-k_x,-k_y}}{F_M}\right)C\left(f_{k_x,k_y}\right)\right]d^3v\right\rangle .$$

The entropy variable associated with fluctuations is also related to $\delta S = S_M - S_m$ in the second order for δf, where $S_M = -\frac{1}{V} \int d^6 Z F_M \ln F_M$ and $S_m = -\frac{1}{V} \int d^6 Z f \ln f$ represent macroscopic and microscopic entropy per unit volume, respectively. The volume in the configuration space is denoted by V.

Our slab ITG turbulence simulations with high velocity-space resolution have confirmed that the quasisteady state, $d(\delta S)/dt \approx \eta_i Q_i$, is realized in a collisionless turbulence with the statistically steady W and Q_i, where monotonic increase of δS is attributed to continuous generation of fine-scale structures of δf by the phase mixing through the parallel advection term [7]. Contrarily, the statistically steady state of turbulence appears in a weakly collisional case, where $\eta_i Q_i \approx -D_i$ and $d(\delta S)/dt \approx dW/dt \approx 0$, and is understood in terms of the production, transfer, and dissipation processes of δS [8]. The steady and quasisteady states are, therefore, represented by two limiting cases of the entropy balance equation.

The phase-mixing processes in a torus are, however, more complicated than that in the slab geometry because of the toroidal magnetic drift and mirror motions as represented in Eq.(1). A power-law decay of a density perturbation, which can be precisely simulated by our toroidal flux tube code [9], is one of the examples. In the next section, we investigate a kinetic damping process of the zonal flow and GAM by means of the gyrokinetic-Vlasov simulation code. Assuming finite k_y modes to vanish, time-evolution of a zonal flow component with $k_y = 0$ (the toroidal mode number $n = 0$) is considered as an initial value problem of a linearized version of Eq.(1). The entropy balance equation is, thus, written as

$$\frac{d}{dt}\left(\delta S_{k_x,0} + W_{k_x,0}\right) = D_{i,k_x,0} \ , \tag{7}$$

which consists of a subset of Eq.(6) with $k_y = 0$. During the collisionless damping of the zonal flow and GAM, thus, $G \equiv \delta S_{k_x,0} + W_{k_x,0}$ is invariant. It is suggested that fine-scale fluctuations of δf should develop in the phase space, while a coherent structure corresponding to the neoclassical polarization can remain in association with the residual zonal flow level.

For precise reproduction of the entropy balance, high velocity-space resolution is necessary, since δS reflects fine-scale structures of δf which can be artificially dissipated in numerical simulations with low resolution. The balance equations, Eqs.(6) and (7), thus, provide a good measure of judging whether the micro velocity-space structures consistent with the turbulent transport are correctly resolved or not.

4. Collisionless Damping of Zonal Flow and GAM

Collisionless damping of the zonal flow components and their residual level is considered to be critical to determination of a saturation level of the ITG turbulent transport [10]. Then, the initial value problem of the zonal flow and GAM, where a response function of a $k_y = 0$ mode is dealt with [10], has been investigated as an important benchmark test of toroidal gyrokinetic simulation codes [14–16]. The collisionless damping of the zonal flow and GAM is caused by the phase mixing processes which generate fine-scale structures of δf in the velocity space. According to Eq.(7), the entropy variable associated with the fine structures should increase during the collisionless decrease of the potential energy. The conservation property given in Eq.(7) and velocity-space profiles of the distribution function are useful for confirming accuracy of the numerical simulations, while they have not been examined in the previous studies.
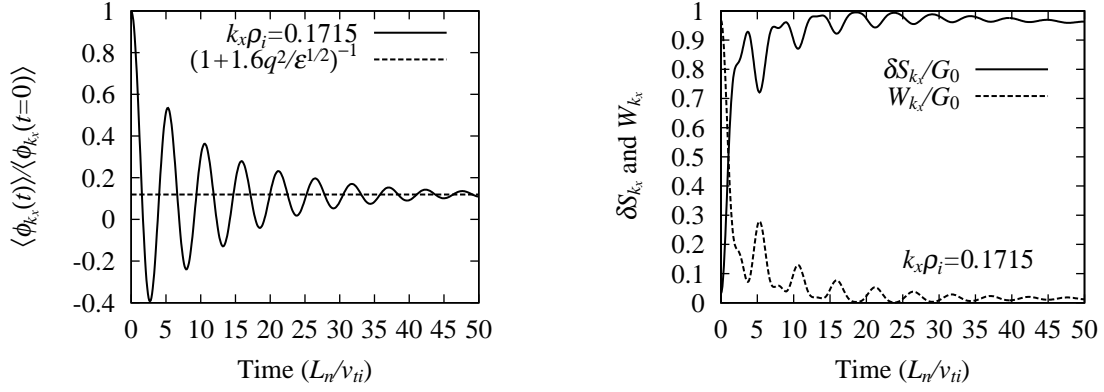
FIG. 1: *Time-evolutions of the zonal flow potential (left), the entropy variable, $\delta S_{k_x,0}$, and the potential energy, $W_{k_x,0}$, (right) obtained by the toroidal flux tube simulation, where $G_0 = \delta S_{k_x,0} + W_{k_x,0}$ at $t = 0$.*
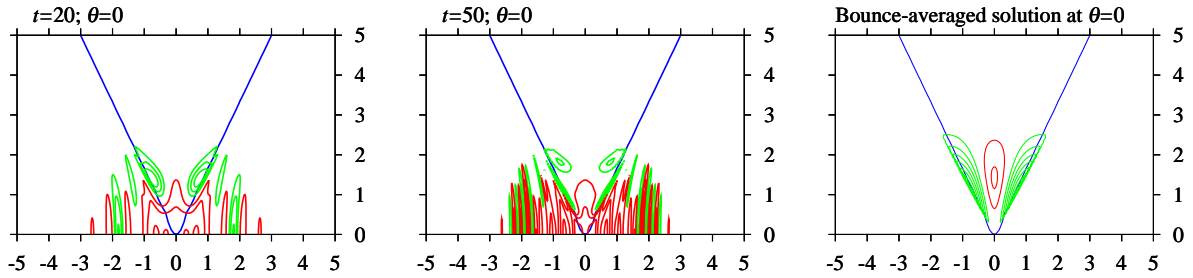

FIG. 2: *Velocity-space profiles of real part of the perturbed distribution function at $\theta = 0$ for different time steps of simulation (left and middle). The bounce-averaged analytical solution is shown in the right panel. The horizontal and vertical axes are defined by $v_\parallel$ and $\sqrt{2\mu\Omega_i}$, respectively, where μ is the magnetic moment. Positive and negative parts are colored by red and green, respectively. Blue lines show the boundary of trapped and passing particles.*

Amplitude of the zonal flow, $\langle \phi_{k_x,0} \rangle$, initially given by the Maxwellian perturbation with $m = n = 0$ decreases as the collisionless damping of GAM oscillation, where m and n mean the poloidal and toroidal mode numbers, respectively. Time-evolution of $\langle \phi_{k_x,0} \rangle$ obtained by the toroidal flux tube simulation for the Cyclone DIII-D base case parameters [14] is shown in Fig.1 (left), where the radial wave number $k_x = 0.1715\rho_i^{-1}$. The used parameters are as follows; $R_0/L_T = 6.92$, $\varepsilon \equiv r_0/R_0 = 0.18$, $r_0/\rho_i = 80$, $\hat{s} = 0.78$, $q_0 = 1.4$, $\eta_i = 3.114$, and $\tau = 1$. The residual level of $\langle \phi_{k_x,0} \rangle$ agrees well with the theoretical estimate, $\lim_{t \to \infty} \langle \phi_{k_x,0}(t) \rangle / \langle \phi_{k_x,0}(t = 0) \rangle = 1/(1 + 1.6q^2/\varepsilon^{1/2})$ [10]. During the collisionless damping of zonal flow and GAM, $\delta S_{k_x,0}$ increases as shown in Fig.1 (right), while the potential energy, $W_{k_x,0}$, decreases to a quite small level. For discretization of the velocity space, $-5v_{ti} \leq v_\parallel \leq 5v_{ti}$ and $0 \leq \mu \leq 12.5v_{ti}^2/\Omega_i$, we have employed 1025×65 grid points, while 128 grid points are used for $-\pi \leq z < \pi$. The high phase-space resolution enables us to reproduce the conservation of G with a relative error less than 3%.

Velocity-space profiles of Re[$f_{k_x,0}$] at different time steps are shown in Fig.2, where the boundary of trapped and passing ions is represented by blue lines. Contribution of the trapped ions to the neoclassical polarization [10] is clearly identified by a mean negative value of $f_{k_x,0}$ for trapped particles. A profile of the distribution function resulting from the numerical simulation agrees with a bounce-averaged analytical solution except for fine-scale oscillations as shown in Fig.2 (right). Generating fine-scale structures of $f_{k_x,0}$ in the direction of the parallel velocity ($v_\parallel$), the phase mixing due to the passing particles largely deforms the initial Maxwellian
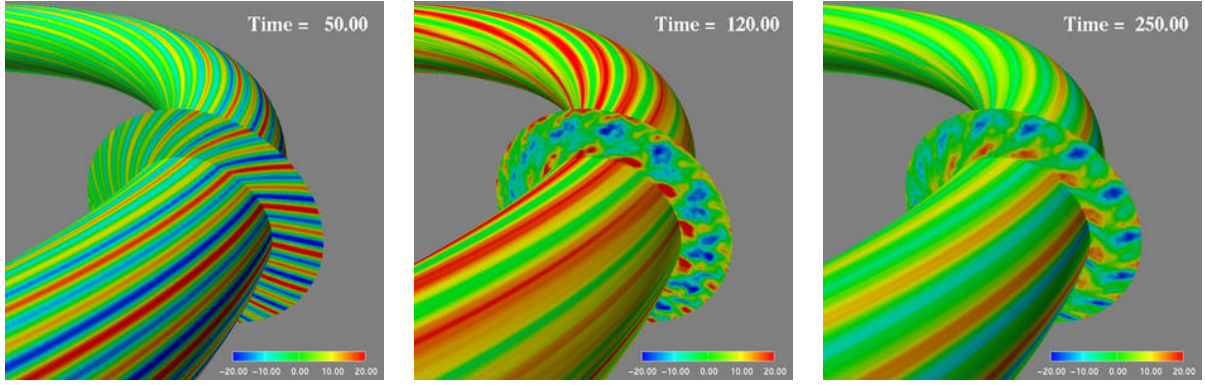
FIG. 3: Color contours of the electrostatic potential obtained by the toroidal ITG turbulence simulation at $t = 50$ (left), 120 (middle), and $250 L_n/v_{ti}$ (right).

distribution as seen in Fig.2, and results in damping of GAM. The increase of $\delta S_{k_x,0}$ balancing with decrease of $W_{k_x,0}$ stems from the development of $f_{k_x,0}$ in the micro velocity-scale, which is revealed by the kinetic simulation with high velocity-space resolution. Diffusion of the fine structures of $f_{k_x,0}$ as well as slow collisional decay of $\langle \phi_{k_x,0} \rangle$ is also confirmed if the finite collisionality is introduced (not shown). Collisionless zonal flow dynamics in helical systems is also investigated based on the gyrokinetic theory and simulation [17].

5. Toroidal ITG Turbulence

Nonlinear gyrokinetic-Vlasov simulations of the toroidal ITG turbulence are carried out by means of the flux tube model described in section 2. The used parameters are the same as those in section 4 but with finite collisionality. A model collision operator with the Lenard-Bernstein form averaged for the gyrophase is introduced, such as

$$C\left(f_{k_x,k_y}\right) = \nu \left[\frac{1}{v_\perp} \frac{\partial}{\partial v_\perp} \left(v_\perp \frac{\partial f_{k_x,k_y}}{\partial v_\perp} + \frac{v_\perp^2}{v_{ti}^2} f_{k_x,k_y} \right) + \frac{\partial}{\partial v_\parallel} \left(\frac{\partial f_{k_x,k_y}}{\partial v_\parallel} + \frac{v_\parallel}{v_{ti}^2} f_{k_x,k_y} \right) - \frac{k_\perp^2}{\Omega_i^2} f_{k_x,k_y} \right] ,$$

(8)

where ν denotes the ion-ion collision frequency.

Color contour plots of the electrostatic potential obtained by the toroidal ITG turbulence simulation are shown in Fig.3 for three different time moments, where $\nu = 10^{-3} v_{ti}/L_n$, $N_\theta = 4$, $k_{x,\min} = 0.1715$, $k_{x,\max} = 5.145$, $k_{y,\min} = 0.175$, and $k_{y,\max} = 1.75$ (31×21 Fourier components are involved in the k_x-k_y space, excluding their complex conjugates as well as modes employed for de-aliasing). The minimum values of k_x and k_y correspond to $\Delta q = 0.5$ and $N_\alpha = 10$, respectively, where Δq denotes a difference of the safety factor across the radial width. The toroidal periodicity of N_α is also assumed [13]. In a latter phase of the linear growth of the ITG instability ($t \approx 60 L_n/v_{ti}$), the zonal flow components are spontaneously excited, and reduce the turbulence level. Vortices with a larger scale than that of the linearly most unstable mode dominate in the turbulence and are mainly responsible for the ion heat transport. A statistically steady turbulence is observed after $t \approx 120 L_n/v_{ti}$ with finite amplitudes of zonal flows.

The entropy balance in the ITG turbulence simulation is shown in Fig.4 (left), where time-histories of four terms in Eq.(6) are plotted. The relative error Δ/D_i in the saturated turbulence after $t \approx 80 L_n/v_{ti}$ is suppressed at 7-8% by use of high resolution, where 960 and 129×48 grid points are employed in the z- and $v_\parallel$-$v_\perp$ space, respectively. Better balancing of Eq.(6) is found for finer grid spacing, Δz, or for higher collision frequency, ν, since fine-scale fluctuations
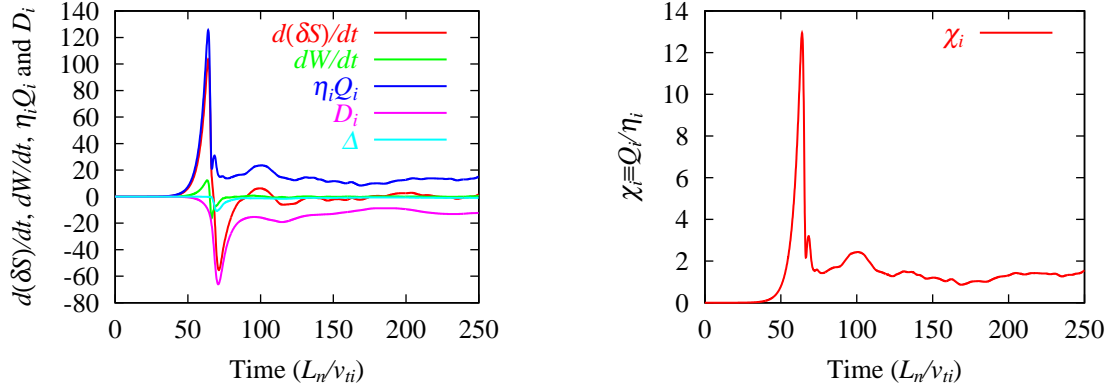
FIG. 4: *Entropy balance (left) and ion thermal transport coefficients χ_i (right) obtained by the toroidal ITG turbulence simulation.*

of δf as well as ϕ are generated in the turbulence. In the steady turbulence, the collisional dissipation nearly balances with the transport flux, $\eta_i Q_i \approx -D_i$, in the same way as seen in the slab ITG simulation [8]. The ion heat transport coefficient, $\chi_i \equiv Q_i/\eta_i$, is shown in Fig.4 (right), where the time-averaged value of $\chi_i \approx 1.4\rho_i^2 v_{ti}/L_n$ from $t = 200$ to $250 L_n/v_{ti}$ in the saturated turbulence is comparable with results of other gyrokinetic simulations for the Cyclone base case ($\chi_i \sim 2\rho_i^2 v_{ti}/L_n$) [14].

The balance of $\eta_i Q_i \approx -D_i$ suggests that fine-scale structures of δf generated by the phase mixing in the turbulence are dissipated by the finite collisionality. Velocity-space profiles of $\text{Re}(f_{k_x,k_y}/\phi_{k_x,k_y})$ observed at $t = 250 L_n/v_{ti}$ are shown in Fig.5 for $k_y = 0.175$ and $0.7\rho_i^{-1}$ where $\theta = z = 0$ and $k_x = 0$. The distribution function of the linear stable mode with $k_y = 0.7$ contains small scale structures in the velocity space, while the velocity-space profile of $\text{Re}(f_{k_x,k_y})$ for the dominant long wavelength mode ($k_y = 0.175$) is similar to that of the linear unstable eigenfunction. This means that the entropy variable produced in the macro velocity-scale by the unstable modes driving the transport is transfered to and is dissipated in the micro scales by the finite collision. It is remarked that the present gyrokinetic-Vlasov simulation with high velocity-space resolution enables one to quantitatively study the entropy balance in the five-dimensional phase space in association with the toroidal ITG turbulent transport, and is also expected to provide detailed information on the distribution function for construction of a toroidal kinetic-fluid closure model [6].

6. Summary

We have studied detailed velocity-space structures of ion distribution functions and related entropy balance in the collisionless damping of the zonal flow and GAM and in the toroidal ITG turbulence, by means of the newly developed toroidal gyrokinetic-Vlasov simulation code with high resolution. The present simulations on the zonal flow and GAM, which accurately satisfy the entropy balance, successfully reproduce the neoclassical polarization of trapped ions as well as the parallel phase mixing due to passing particles. During the collisionless damping of GAM, finer-scale structures of the distribution function in the velocity space continue to develop due to the phase mixing while preserving an invariant defined by a sum of the entropy variable and the potential energy. Thus, the collisionless dynamics of the zonal flow and GAM are comprehended in terms of a transfer process of the entropy variable from macro to micro velocity-scales.
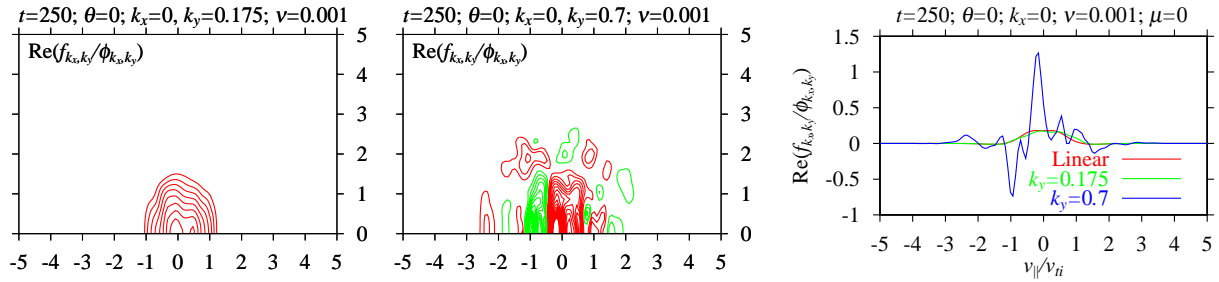
FIG. 5: *Velocity-space profiles of real part of the perturbed distribution function observed in the toroidal ITG turbulence simulation at $t = 250 L_n/v_{ti}$ for $k_y = 0.175$ (left) and $0.7 \rho_i^{-1}$ (middle) where $\theta = z = 0$ and $k_x = 0$. The horizontal and vertical axes are defined by $v_\parallel$ and $\sqrt{2\mu\Omega_i}$, respectively. The cross-sectional plots at $\mu = 0$ are shown in the right panel where the linear eigenfunction for $k_y = 0.175$ is also given for comparison.*

Simulation results of the anomalous transport in the toroidal ITG turbulence, in attention to the velocity-space structures of the distribution function and the entropy balance, are also presented. The heat transport flux in the statistically steady turbulence is mainly produced by vortices with long wavelengths, while fine velocity-space structures of the perturbed distribution function clearly appear in fluctuations with larger wavenumbers. Accordingly, the entropy variable produced by the unstable modes with long wavelengths is transfered in the wave number and velocity spaces, and is dissipated by the finite collision. Thus, the statistically steady turbulence is sustained, where the growth of the entropy variable and the potential energy is saturated with a balance between the transport flux and the collisional dissipation.

Reference

[1] HORTON, W., Rev. Mod. Phys. **71**, 735 (1999).
[2] TERRY, P.W., Rev. Mod. Phys. **72**, 109 (2000).
[3] DIAMOND, P.H., ITOH, S.-I., ITOH, K., HAHM, T.S., submitted to Plasma Phys. Contl. Fusion (2004).
[4] KROMMES, J.A., HU, G., Phys. Plasmas **1**, 3211 (1994).
[5] SUGAMA, H., OKAMOTO, M., HORTON, W., WAKATANI, M., Phys. Plasmas **3**, 2379 (1996).
[6] SUGAMA, H., WATANABE, T.-H., HORTON, W., Phys. Plasmas **8**, 2617 (2001).
[7] WATANABE, T.-H., SUGAMA, H., Phys. Plasmas **9**, 3659 (2002).
[8] WATANABE, T.-H., SUGAMA, H., Phys. Plasmas **11**, 1476 (2004).
[9] WATANABE, T.-H., SUGAMA, H., to appear in J. Plasma Fus. Res. SERIES **6** (2004).
[10] ROSENBLUTH, R.M., HINTON, F.L., Phys. Rev. Lett. **80**, 724 (1998).
[11] WINSOR, N., JOHNSON, J.L., DAWSON, J.J., Phys. Plasmas **11**, 2448 (1968).
[12] FRIEMAN, E.A, CHEN, L., Phys. Fluids **25**, 502 (1982).
[13] BEER, M.A., COWLEY, S.C., HAMMETT, G.W., Phys. Plasmas **2**, 2687 (1995); BEER, M.A, Ph.D thesis, Princeton University, 1994.
[14] DIMITS, A.M., et al., Phys. Plasmas **7**, 969 (2000).
[15] LIN, Z., et al., Phys. Plasmas **7**, 1857 (2000).
[16] CANDY, J., WALTZ, R.E., J. Comput. Phys. **186**, 545 (2003).
[17] SUGAMA, H., WATANABE, T.-H., Proceedings of the 12th International Congress on Plasma Physics (Nice, France, 2004), 084 & P2-100 (topic D).